



## ZnO/polyaniline composite based photoluminescence sensor for the determination of acetic acid vapor

Mehmet Turemis<sup>a,\*\*</sup>, Daniele Zappi<sup>a</sup>, Maria Teresa Giardi<sup>a,b</sup>, Giovanni Basile<sup>a</sup>, Almira Ramanaviciene<sup>c</sup>, Aleksandrs Kapralovs<sup>d</sup>, Arunas Ramanavicius<sup>c,\*</sup>, Roman Viter<sup>d,e,\*\*\*</sup>

<sup>a</sup> Biosensor Srl, Via Degli Olmetti 44, 00060, Formello Rome, Italy

<sup>b</sup> Istituto di Cristallografia, CNR Area Della Ricerca di Roma, 00015 Monterotondo Scalo Rome, Italy

<sup>c</sup> Vilnius University, Faculty of Chemistry and Geosciences, Institute of Chemistry, Naugarduko g. 24, Vilnius, 03225, Lithuania

<sup>d</sup> University of Latvia, Institute of Atomic Physics and Spectroscopy, 19 Rainis Blvd., Riga, LV, 1586, Latvia

<sup>e</sup> Sumy State University, Center for Collective Use of Research Equipment, 31 Sanatorna Street, 40000, Sumy, Ukraine

### ARTICLE INFO

#### Keywords:

Photoluminescence  
ZnO-PANI composite  
Gas sensor  
Acetic acid  
Cellulose degradation  
Conducting polymers

### ABSTRACT

In this study, we report a novel ZnO/polyaniline (PANI) nanocomposite optical gas sensor for the determination of acetic acid at room temperatures. ZnO nanorods, synthesized in powder form were coated by PANI (ZnO/PANI) by chemical polymerization method. The obtained nanocomposites were deposited on glass substrate and dried overnight at room temperature. Structure and optical properties of ZnO/PANI nanocomposite have been studied by using X-ray diffraction, transmission electron microscopy, scanning electron microscopy, diffuse reflectance and photoluminescence spectroscopy. Tests towards acetic acids were performed in the range of concentrations 1–13 ppm. The adsorption of acetic acid on the sensor's surface resulted in the decrease of ZnO/PANI photoluminescence. The response and recovery time of the sensor were in the range of 30–50 s and 5 min, respectively. The developed sensors showed sensitivity towards acetic acid in a range of 1–10 ppm with the limit of detection of 1.2 ppm. Specially designed miniaturized sensing system based on integrated sensing layer, light emission diode as excitation source and optical fiber spectrometer was developed for the measurement of the sensor signal. The developed sensing system was applied for the investigation of some real sample assessment including the evaluation of storage conditions of ancient cellulose acetate films, which during the degradation are releasing acetic acid. The obtained results suggest that the developed novel optical ZnO/PANI nanocomposite based sensor shows great potential for acetic acid determination in various samples.

### 1. Introduction

Sensing of small organic volatile compounds is an important issue in sensor development. Numerous small organic molecules are dangerous for human health or interfere severely in numerous industrial productions [1]. Acetic acid is a corrosive substance that is used in numerous industrial applications and hence it is present, mainly as vapor, in some industrial atmospheres. It is the principal constituent of the volatile acidity of wines and vinegars. It is also traditionally used as an oxidizing agent in organic synthesis [2]. On another hand, acetic acid is an important compound for the monitoring of cellulose acetate films [3]. A huge percentage of the recent cultural heritage can be found in movies, photographs, posters and slides produced between 1895 and 1970 were

made using cellulose derivate [4,5]. More than 75 years of visual and audio memories are in serious danger to be lost due to the natural instability of cellulose acetate. The degradation produces acetic acid (vinegar effect), in an autocatalytic process [5]. Thus, it is important to have sensors able to detect the presence of acetic acid and to control its concentration over time in order to be able to take preventive actions for human health and heritage preservation [5].

In past decades, some gas sensors for the determination acetic acid have been developed [6,7]. Quartz crystal microbalance (QCM) based sensors, coated with polyaniline (PANI) layers were used for the determination of acetic acid [3]. The sensors were suitable for the measurement of acetic acid concentrations in a wide range but irreversible changes of signal response were observed over time. The same

\* Corresponding author.

\*\* Corresponding author.

\*\*\* Corresponding author. University of Latvia, Institute of Atomic Physics and Spectroscopy, 19 Rainis Blvd., Riga, LV, 1586, Latvia.

E-mail addresses: [m.turemis@biosensor.it](mailto:m.turemis@biosensor.it) (M. Turemis), [arunas.ramanavicius@chf.vu.lt](mailto:arunas.ramanavicius@chf.vu.lt) (A. Ramanavicius), [roman.viter@lu.lv](mailto:roman.viter@lu.lv) (R. Viter).

irreversible changes were observed in optical sensors, based on PANI [8]. Therefore, such sensors were very inaccurate and/or needed very frequent recalibration [3,8].

In another research, it was demonstrated that Poly[2-methoxy-5-(2-ethylhexyloxy)-1,4-phenylenevinylene] (MEH-PPV) based films can be used as fluorescent probes for acetic acid vapor detection [9] and therefore such layers probably are suitable for the determination of acetic acid. However, these sensors require a high-intensity light source for photoluminescence (PL) excitation and show lower sensitivity compared to PANI-based layers sensors. Furthermore, sensor stability over time and use is also a concern since these films undergo photo-degradation. Therefore, practical application of sensors based on such layers is very limited.

Considerable attention in recent years has been directed to sensors for toxic gases based on metal oxide semiconductors. Among many others, zinc oxide (ZnO) is a unique material, which possesses specific semiconducting and optical properties. Many different nanostructures based on ZnO are known, all of them have very high surface area compared to their geometrical area. Such extended ZnO surface area is very important for the application in sensing and biosensing devices [3]. Zinc oxide has a wide band gap, which depends on doping and/or the number of defects in the crystal structure of ZnO [1]. This semiconducting material shows good applicability in catalytic and sensing devices [2,3,10,11].

In addition to attractive physicochemical properties, zinc oxide is non-toxic and possess good biocompatibility, which makes this material even more attractive for sensor development [3]. Till now, few studies have been carried out regarding the acetic acid sensing characteristics of ZnO nanoparticles. Some sensors utilize doped semiconducting metal oxide nanolayers, with detection based on resistance measurements [6,7]. The principle of action of such sensors is based on the catalytic degradation of acetic acid on the doped metal nanostructured surface. However, the most common metal oxide semiconductors sensitive to gases are n-type semiconductors, thus, they demand high operating temperatures that limits their use at room temperature. Particularly, the resistance of metal oxide based sensors for acetic acid at 120–400 °C depends on the type of metal oxide and the doping. In particular, a correlation between concentration of acetic acid and variation in measured resistance of the sensor has emerged [6,7].

Therefore, novel analytical and/or bioanalytical methods, which overcome current state-of-the-art and enable fast, sensitive, specific and high-throughput detection, are in great demand.

The photoluminescence of ZnO is very attractive for sensor development operating at room temperature because, once properly functionalized, ZnO can be exploited as a selective analytical transducer, which enables to enhance the analytical signal, increase detection sensitivity and signal-to-noise ratio [3–8].

In the present work, we report novel ZnO/PANI nanocomposite based photoluminescence sensors for the determination of acetic acid vapors at room temperatures. The main sensors parameters (sensitivity, selectivity, limit of detection, response and recovery time, etc.) are discussed. Integration of the ZnO/PANI nanocomposites with portable optical system for application in vinegar analysis and in cultural heritage protection has been demonstrated.

## 2. Materials and methods

### 2.1. Materials and consumables

Aniline monomer (CAS Number: 62-53-3), ethanol (CAS Number: 64-17-5) and hydrogen peroxide (30%) (CAS Number: 7722-84-1), pure acetic acid (98%) (CAS Number: 64-19-7) were purchased from Sigma Aldrich. Mili-Q water was used in all experiments.

### 2.2. ZnO deposition and formation of ZnO-PANI composite

Indium thin oxide coated glass plate was used as solid support. ZnO nanorods were deposited as powder by gaseous disperse method as explained in previous methods [12]. PANI was synthesized by oxidative-chemical deposition method [13]. The 1 mg/ml of ZnO nanorod (ZnO-NR) colloidal suspension in water was mixed with pure aniline. 50 mM and 200 mM aniline concentrations were used for composite preparation. The solution was rigorously stirred and treated by ultrasound for 15 min. Then an oxidizing agent – hydrogen peroxide – was added. The synthesis was performed at room temperature for 8 h.

In order to prepare sensing layer, glass substrates 10 mm × 10 mm were cleaned in isopropanol and dried at room temperature. Twenty microliters of the ZnO-PANI composite solution were deposited on the prepared glass by drop casting method and then dried overnight.

### 2.3. Characterization techniques

Structural properties of ZnO-PANI nanocomposites have been investigated by X-ray diffraction spectroscopy (XRD) on a Rigaku Ultima XRD-setup (CuK $\alpha$ ,  $\lambda$  = 0.154 nm). Conventional powder diffraction analysis was performed by acquiring the  $\theta$ -2 $\theta$  spectra in the  $\theta$  range from 20 to 80°. The surface morphology of the samples was determined using TESCAN scanning electron microscope (SEM) and high resolution transmission electron microscopy (HRTEM) Tecnai GF20 from FEI (Eindhoven, The Netherlands). Room temperature photoluminescence spectra of ZnO-PANI nanocomposites were studied in the range of 360–800 nm using light emitting diode (LED) ( $\lambda$  = 340 nm, 0.4 mW output power) and Ocean optic (USB4000) spectrometer for excitation and registration of photoluminescence. Reflectance measurements were performed by using Ocean optic (USB4000) spectrometer and halogen-deuterium light source (Ocean Optics).

### 2.4. Experimental setup for gas sensing

The experimental laboratory setup for gas sensing is shown in Fig. 1A. The setup is mounted on an optical table rail. Light emitting diode (LED) was used as an excitation source. The band pass filter with

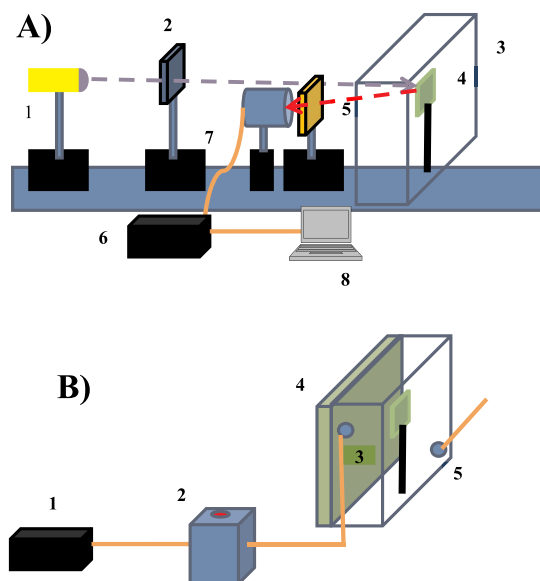


Fig. 1. Experimental setup for gas integrated sensing scheme (A) based on: LED (1), band pass filter (2), gas chamber (3), sample holder (4), long pass filter (5), detector (6), lens (7), computer (8) and gas supply system (B) showing air pump (1), buffer volume (2), inlet chamber (3), measurement cell (4) and outlet (5).

transmittance in the range of 320–380 nm was used to cut off noise green emission from LED. The gas chamber made of plastic was equipped with a sample holder. The emitted light was passed through long pass filter 5 with transmittance in the range of 370–900 nm to cut off a signal from LED. The signal was collected with fiber optic spectrometer Ocean Optics USB4000, equipped with collimating lens fixed on the tip of 600  $\mu\text{m}$  core multimode optical fiber. Measurements were performed in dynamic regime with SpectraSuite software.

Gas supply system is shown in Fig. 1B. Air pump with a fixed pumping speed (50 l/h) was connected with a buffer volume. The probe was introduced into the inlet chamber filled with 4 ml of buffer solution and then it was pumped into the measurement cell, which was of 60 ml volume. The gas was removed from the measurement cell through outlet. The measurement cell was equipped with transparent quartz glass (green colored) to transmit excitation and emission lights.

Several wavelengths from PL spectra of ZnO/PANI were selected for kinetic measurements. As result, PL intensity at the fixed wavelengths was analyzed before and after exposure towards gas. Pure acetic acid (98%) was added to the buffer volume 2 in the range of 0.25–2  $\mu\text{L}$ . Concentration of acetic acid was calculated according to literature corresponding to 1–13 ppm [3].

Miniature prototype of the integrated system was built up using newly designed measurement cell (made in black delrin) that can hold sensing layer, excitation light (LED with wavelength 340 nm and output power 0.4 mW), filter and optical fiber required for the measurement of the emitted photoluminescence. The measurement cell allows exposure to the acetic acid on the surface of the sensing layer through an inlet and outlet (Fig. 2C). The PL of ZnO/PANI surface was excited by 340 nm wavelengths. PL integration time was 5 s.

### 2.5. Measurements of cellulose acetate by indicators strips

A-D Strips (RIT Image Permanence Institute, UK) are dye-coated paper strips that detect and measure the severity of acetate film deterioration, vinegar syndrome, in film collections. When placed inside a

closed system for 24 h the change color in the presence of the acidic vapor given off by degrading film. As the level of acidity increases, they change from their original blue color (0: no deterioration) through blue-green (1: deterioration starting), green (2:actively degrading), and finally to bright yellow (3 critical degrading).

## 3. Results and discussion

### 3.1. Structural properties of ZnO-PANI nanocomposites

The XRD patterns obtained for ZnO and ZnO/PANI nanocomposite are presented in Fig. 3A. The 50 mM concentration of aniline didn't provide conformal coating (data not shown) therefore all the experiments performed with composite material obtained by 100 mM aniline coating. XRD spectrum of ZnO nanorods showed reflection peaks related to ZnO at  $2\theta$  31.6°, 34.3°, 36.1°, 47.4°, 56.4°, 62.7° and 67.8° [14]. The observed peaks correspond to the reflections from the next crystal planes: (100), (002), (101), (102), (110), (103), (112) and (004) respectively which were similar to that reported previously [14]. PANI layer deposited on ZnO surface quenches some of XRD peaks, related to ZnO. New peaks at 25.88, 27.08, 28.83° were attributed to PANI peaks, related to (200), (121) and (022) PANI crystallographic planes [15]. The XRD peaks point the forming of crystalline conductive PANI in the form of emeraldine salt [15]. Peaks of ZnO at 55.88, 60.2 and 64.88 are shifted due to forming of ZnO/PANI composite structure [16].

Scanning electron microscopy (SEM) image of the ZnO/PANI on a glass substrate Fig. 3B shows a uniform distribution of nanostructure grains of about 60–90 nm diameter and 400–600 nm length. The dimensions of ZnO nanorods after PANI deposition slightly increased, comparing to that reported in other researches [14,17]. Fig. 3C shows HRTEM image of the ZnO/PANI indicating, conformal coating of PANI. The average thickness of the PANI coating, estimated from HRTEM image was estimated  $7 \pm 3$  nm.

50 mM and 200 mM aniline concentrations were used for composite preparation. The lower concentration do not provided conformal

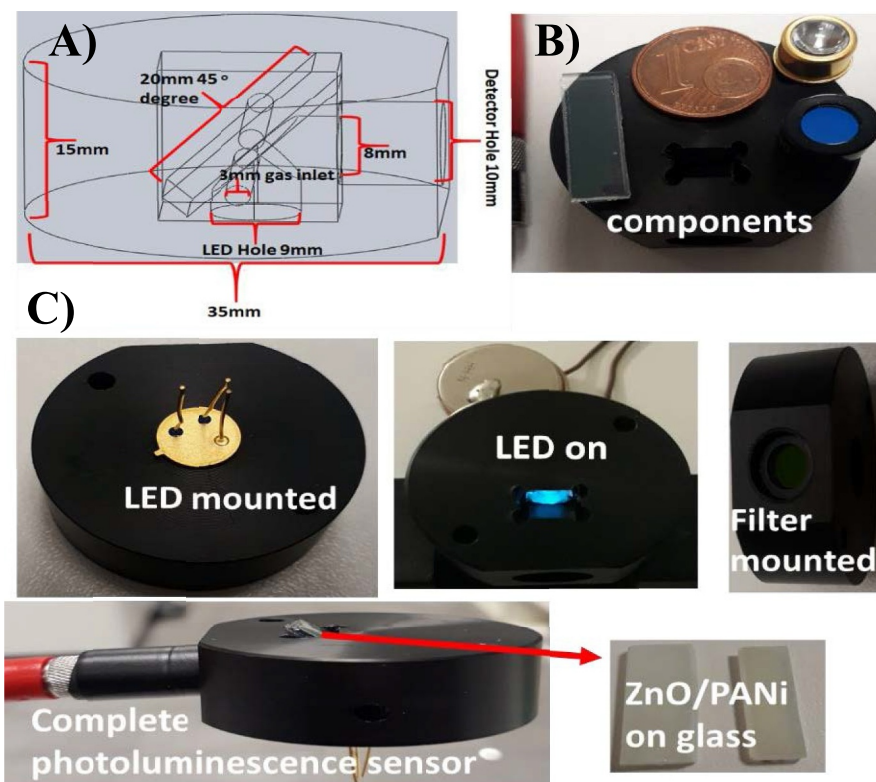


Fig. 2. A) Drawings of the measurement chamber indicating the angle of measurement of photoluminescence by the fiber optic spectrometer Ocean Optics USB4000, B) parts of the developed sensor array, C) in order from left: LED mounted on measurement cell, measurement cell when UV LED turned on, filter mounted on measurement cell, complete sensor assembly with glass plate deposited ZnO/PANI sensing layer.

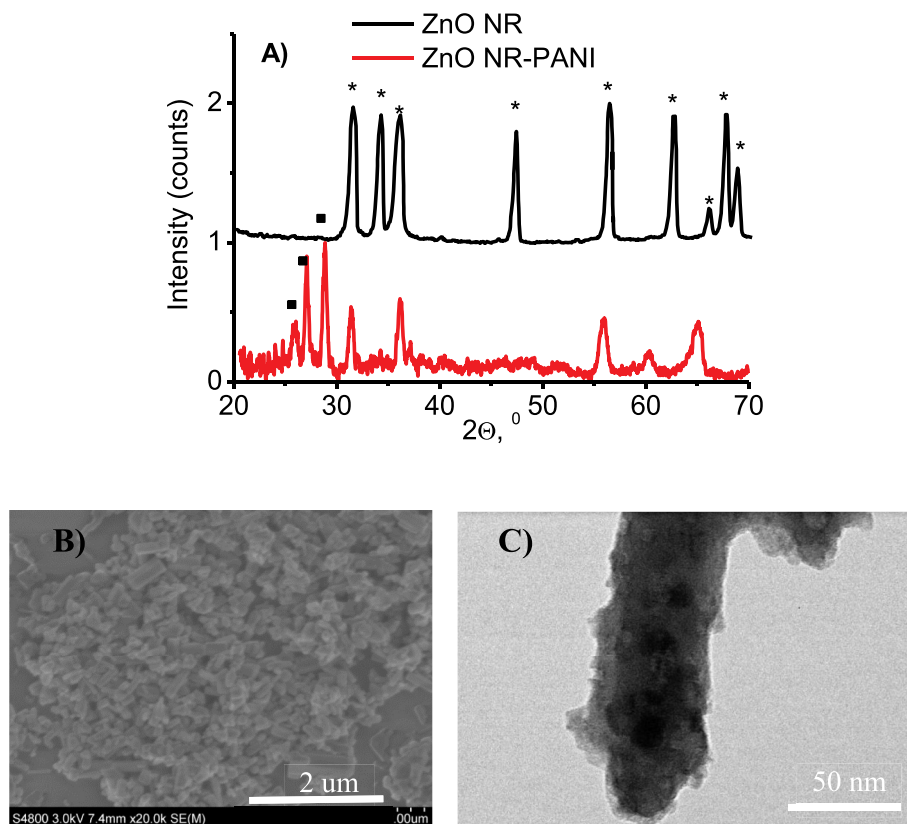


Fig. 3. Structural characterization of ZnO/PANI nanocomposite: (A) XRD spectra of the ZnO nanorods and ZnO/PANI nanocomposite (ZnO and PANI peaks are marked as \* and ■, respectively), SEM image (B) and HRTEM image (C) of ZnO/PANI nanocomposite.

coating but the higher concentration significantly quenched PL of ZnO, what is in line with similar effect observed for interaction of some other photoluminescence exhibiting materials with other conducting polymer – polypyrrole [18,19].

### 3.2. Photoluminescence measurements

Optical properties of ZnO/PANI nanocomposite were evaluated after the deposition of this composite on glass slide. Fig. 4A shows diffuse reflectance spectra of ZnO nanorods before and after PANI deposition. It was seen, that the absorption edge of ZnO/PANI has shifted towards UV region compared to ZnO nanorods. It points the charge transfer from PANI to ZnO in formed ZnO/PANI nanocomposites [16]. In addition, two absorption edges appeared in ZnO/PANI spectra in the range of 470 and 700 nm. The observed peaks correspond to PANI absorption peaks [20]. According to the literature [20], PANI nanostructures have broad absorption peak at 325 nm with full width of half maximum ~ 60 nm. It points that PANI absorption might overlap with ZnO emission in UV and visible ranges.

Photoluminescence spectra of ZnO NRs before and after PANI deposition are shown in Fig. 4B. PANI deposition results in a decrease of intensity of ZnO-based PL. Sufficient decrease of PL emission might be related to absorption of the emitted light by PANI. Peak shifts are observed in UV and visible region, suggesting the formation of composite with charge transfer between PANI and ZnO. We suppose, that PANI formation on the surface of ZnO might passivate surface centers of non-emission recombination and forming additional bonds with ZnO.

ZnO/PANI PL spectra were excited by LED with wavelength of 340 nm at output power 0.4 mW. The obtained PL spectra were different from that reported in other research based on bare ZnO layers not modified by PANI [14]. PL intensity of ZnO nanostructures is

significantly dependent on the excitation power [21]. For UV peak of ZnO (mainly free excitons) this dependence is superlinear, whereas for Vis peak of ZnO (mainly defect emission) it remains sublinear [21]. Therefore, by using single 340 nm LED there is a risk of suppression of PL intensity, but at the same time the increase of noise-to-signal ratio is observed. In this context, further kinetic measurements of the sensor prototype were performed only at fixed 380 nm and 520 nm wavelengths, where the best PL performance has been determined.

### 3.3. Evaluation of sensor response towards acetic acid

A miniaturized (5 × 5x6 cm) prototype of the optical sensing system was developed (Fig. 2C). The sensor is composed by a black derlin cell with a UV LED mounted on a proper filter, exciting the ZnO/PANI sensing layer on glass. The emission of photoluminescence activity is read by an optical fiber at 90°.

The presence of acetic acid into the measurement cell resulted in the decrease of the PL intensity of ZnO/PANI nanocomposites (Fig. 4C). The kinetic study of adsorption/desorption of acetic acid on the surface of ZnO/PANI is summarized in Fig. 5 A and 5B. Results shows that the intensity of the PL emission peaks decreased when the acid concentration has increased.

Sensitivity of the sensor was calculated using following equation [22]:

$$S = \frac{I_0 - I_{(C)}}{I_0} \quad (1)$$

where  $I_0$  and  $I_{(C)}$  are intensities of emission before and after acetic acid exposure respectively. The calibration curve of the ZnO gas sensor depicts the linear behavior of the sensor response at the measured range of the acetic acid concentrations Fig. 5C and 5D. Limit of detection for the

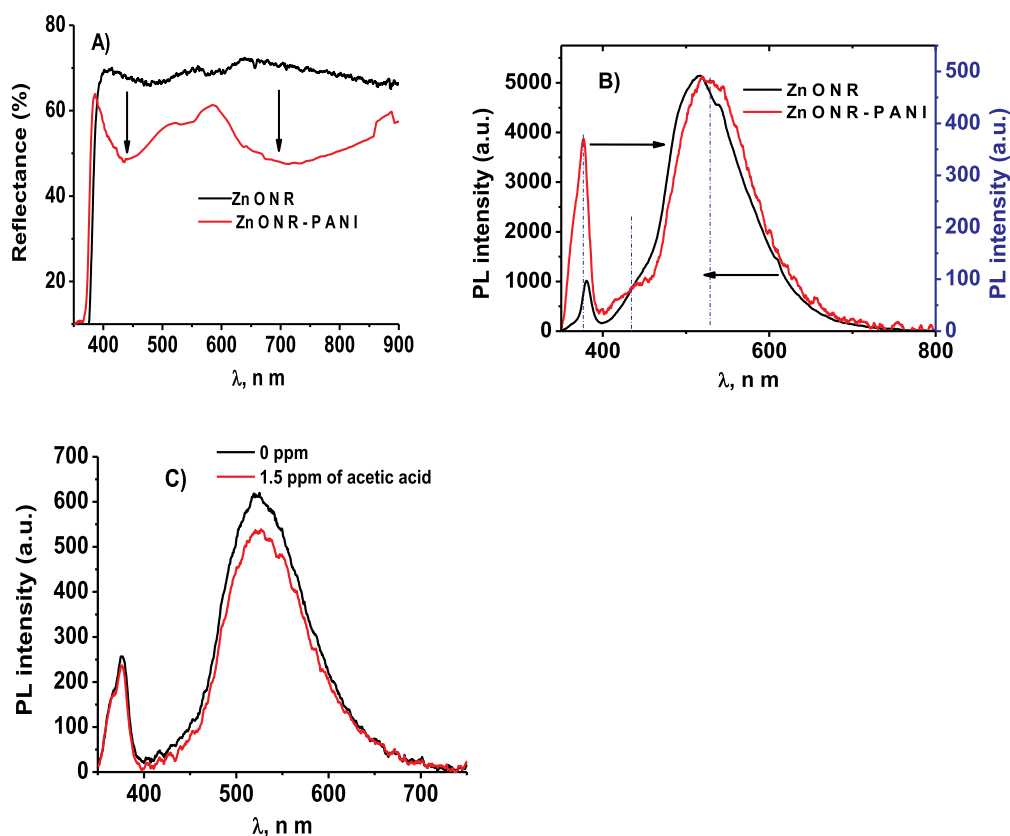


Fig. 4. Optical characterization of ZnO nanorods and ZnO/PANI nanocomposites: Diffuse reflectance spectra of ZnO nanorods and ZnO/PANI composite (A), Photoluminescence spectra of ZnO nanorods and ZnO/PANI nanocomposite (B), PL spectra of ZnO/PANI nanocomposites before and after injection of acetic acid (C).

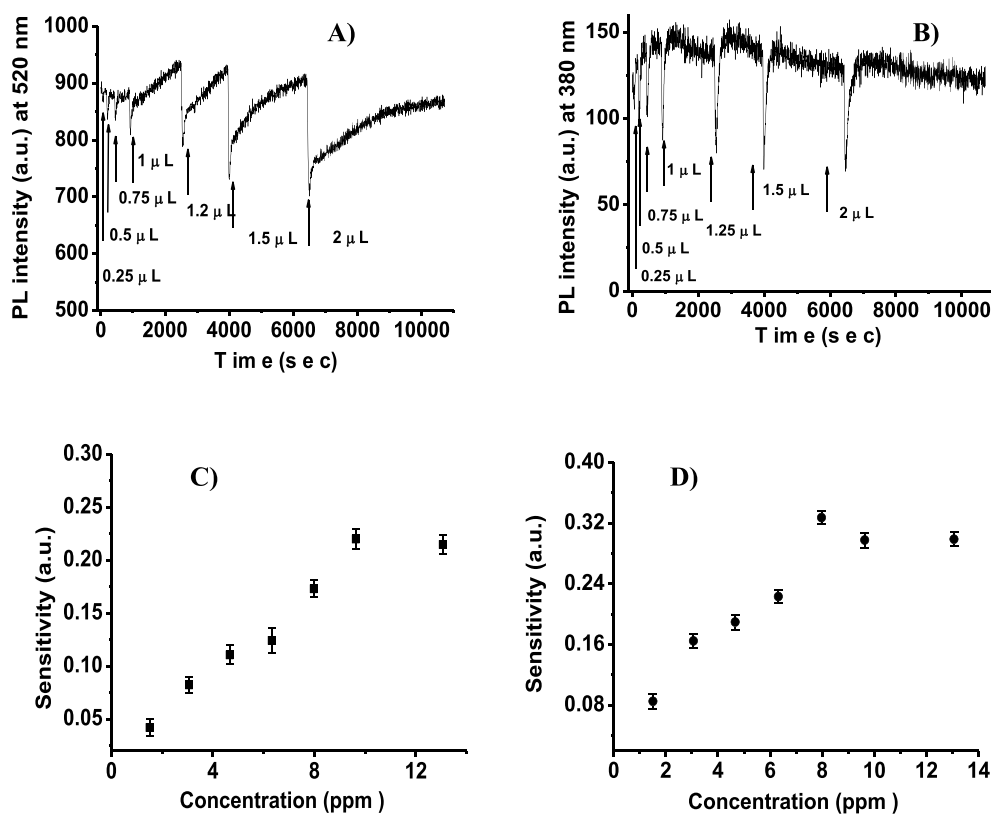


Fig. 5. Dynamic response of the sensor to stepwise exposure and recovery cycles of the increased acetic acid vapors at 520 nm (A) and 380 nm (B), and obtained calibration curves at 520 nm (C) and 380 nm (D).

sensor was calculated using the following equation [22,23]:

$$LOD = \frac{3\sigma}{K} \quad (2)$$

where  $\sigma$  and  $K$  are standard deviation and a slope of linear part of the sensitivity plot, respectively. The obtained LOD values were 2 ppm and 1.2 ppm for 380 and 520 nm peaks. Difference in sensitivity is related to the PANI layer and their optical properties. Due to interaction with acetic acid partial oxidation might take place that results in change of optical absorption and of PL signal of the sensor.

It is important to explore sensing principle and underlying reasons for the improved sensing properties of the ZnO/PANI composite structure. The response of the composite, when exposed to acetic acid, can be attributed to the physicochemical properties of PANI and its interaction with ZnO nanomaterials. The proposed sensor is based on the interaction between PANI and acetic acid, which involves a process of physical adsorption and chemisorption of acetic acid over PANI. It is followed by the photooxidation of acetic acid by ZnO-PANI composite and oxidation of PANI due to interaction with acetic acid. There are some studies reporting that enhanced sensitivities for acids or bases may be due porous structure of PANi/ZnO films, leading to the predominance of surface phenomena over bulk material phenomena [3,8,24–26] explained the increase in sensitivity of PANI-ZnO composite by the interference of molecular dimension factor of PANI particle size, providing more surface area to interact with the gas vapor [26]. Several studies explained the enhancement of the response magnitude of inorganic/inorganic or organic/inorganic nanocomposites based on p/n junction theory. They also claimed that the depletion layer established at the interface between ZnO and PANI might result in the decrease of the activation energy and enthalpy of physisorption for target gases, being conducive to better sensing [27]. The common idea is that the increase in the response magnitude of the composites should be due, more than to the increased specific surface area of nanostructures, to the formation of p/n junction between p-type HCl doped polyaniline thin film and n-type ZnO semiconductor. The appearance of a variety of p-n semiconductor contacts likely facilitates the formation of various molecular adsorption sites on the polyaniline surface thus the sensitivity is increased as compared to pure ZnO or polyaniline [24,26,28]. We suppose that acetic acid detection occurs due to interaction between NH<sub>2</sub>- groups and the target molecules. As result, electric field is formed on the surface, which increase depletion width and move electrons from emission centers to the surface. As result, PL intensity decreases.

We also studied response and recovery time of the sensor with respect to acetic acid vapor exposure. From Fig. 5A and B it can be seen

that the sensor signal was partially reversible. Drift of the sensor signal is observed at higher concentrations of acetic acid. Sensor reaches 90% of its saturation value from the initial value in 30 s after exposure to acetic acid vapor. Recovery time of the sensor increases from 215 to 360 s, proportional to the acetic acid concentration in the tested range. The larger recovery times are likely due to the slow rate of diffusion and desorption of acetic acid from the sensing surface.

#### 3.4. Stability, repeatability and selectivity of the sensor

In order to allow long-term measurements, it is desirable that ZnO/PANI sensing layer is retained on the glass without any significant loss of activity over long periods. Thus, the stability of the deposited ZnO/PANI layer was tested by measuring the photoluminescence activity for 40 days by exposing 5 ppm acetic acid vapor. The sensor retained approximately 98, 95, 94 and 85% of its initial PL-based response toward acetic acid after 3, 10, 20 and 40 days respectively, when stored at room temperature (25 °C). Significant loss (30%) of the photoluminescence response was observed only after 40 days. Thus, it can be concluded that the sensor could be efficiently used up to 30 days.

Operational stability of the sensor system was studied over 10 h. Measurements were performed every 30 min with integration time 15 s and 40 repetitions. The signal changes show an average value of the signal and standard deviation for 380 nm and 520 nm of  $12219 \pm 176$  and  $1107 \pm 29$  counts, respectively (Fig. 6A). Relative change of the sensor signal after continuous interaction with acetic acid was also tested. The developed sensor is resistive against low concentrations of acetic acid (1–13 ppm). The signal drops up to 20% when exposed to concentrations of acetic acids over 20 ppm.

The reproducibility and repeatability of the proposed acetic acid gas sensor were evaluated by photoluminescence measurements. The glass plates containing deposited sensing layer were prepared independently at different days showing an acceptable reproducibility with relative standard deviations (RSD) of  $0.8 \pm 0.1$  for each 5 ppm of acetic acid vapor determination. The RSDs for each 5 ppm measurements ( $n = 6$ ) were  $0.6 \pm 0.08$  for developed gas sensor revealing the good repeatability of the proposed system.

The sensor selectivity was tested by exposing it to water vapors and 100 ppm ethanol. No signal changes were observed when they were added into the chamber. These results indicate that ZnO/PANI composite based sensor is resistive to water vapor and can successfully distinguish acetic acid over ethanol Fig. 6B.

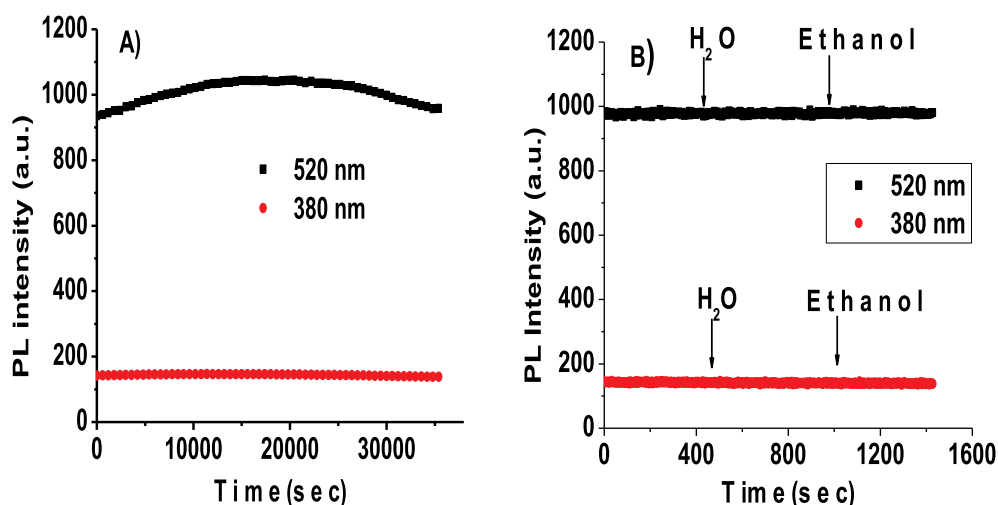


Fig. 6. Operational stability of the sensor signal (A) and response of the sensor to saturated water (over deionized water) and ethanol (over 96% ethanol solution) vapors at 520 nm and 380 nm (B).

**Table 1**

Summary of acetic acid detection by the developed sensor in vinegar and deteriorated cellulose acetate films. The data are average of three determinations  $\pm$  RSD.

Samples	Value found with A-D strips	Value found with described sensor system	Recovery
Vinegar (Cirio; Label value 6%)	–	5.7% $\pm$ 0.4	94.7%
Vinegar (Panorama; Label value 7%)	–	6.4% $\pm$ 0.5	92.1%
Film 1 (No deterioration)	0 (< 1 ppm)	Nr	–
Film 2 (Deterioration started)	1 (1–2 ppm)	1,5 ppm $\pm$ 0.3	–
Film 3 (Actively degrading)	2 (6–8 ppm)	7,6 ppm $\pm$ 0.8	–

Nr.: Not revealed.

**Table 2**

The comparison of the proposed sensor with the previously reported ones based on the utilization of different methods.

Sensing layer	Pr-doped ZnO	poly[2-methoxy-5-(2-ethylhexyloxy)-1,4-phenylenevinylene]	Y-doped SnO <sub>2</sub>	Ni <sup>2+</sup> -doped ZnO	CBF containing CTAB and SNARF-1	ZnO/PANI composite
Analyte	Acetic acid	Formic acid	Acetic acid	Acetic acid	Acetic acid	Acetic acid
Technique	Resistive	PL	Resistive	Resistive	PL	PL
Linear/Working range	20–400 ppm	0–2500 ppm	10–500 ppm	0.001–10 ppm/ 10–1000 ppm	3–65 ppb	1–10 ppm
LOD	N.R	348 ppm	Not reported	0.001 ppm	3ppb	1.2 ppm
Operating temperature	200–375 °C	R.T	300 °C	310 °C	RT	R.T
Response time	37–51s	18s	4–7s	4s	N.r.	30s
Recovery time	48–40s		8–11s	27s	N.r.	215–360s
Partial selectivity over	Methanol, DMF	Nr	Ammonia, DMF Methanol	Benzene Toluene	SO <sub>2</sub>	Ethanol
Reference	[30]	[9]	[7]	[31]	[32]	Present work

N.r – not reported

### 3.5. Real sample analysis

We applied the sensor to the monitoring of acetic acid in real samples. The proposed method was applied for the determination of acetic acid concentrations in two commercial vinegar samples from the local market. The concentrations of acetic acid in commercial vinegar and produced by film samples (average of three determinations) were measured using the proposed sensor Table 1. Using the calibration curve, the acid concentration of the commercial vinegar samples was found to be around 6–7%. Obtained results are in line with by producer declared acetic acid concentration.

Another application of ZnO/PANI-based sensor, which was tested in this research, was related to the determination of acetic acid arising during the degradation of cellulose acetate, which is used in ancient films. Acetic acid gas arising from ancient film samples was measured after 1 h incubation of the films with the gas sensor in a sealed box.

The results summarized in Table 1 were in good agreement with the results obtained with A-D strips. These are filter paper strips soaked with a pH colorimetric indicator, which are placed inside the film box and incubated for 24 h. By reacting with the acetic acid produced by the film degradation, the pH indicator in the strips changes color. After the incubation, the degradation level is evaluated by comparing the color of the strips with a provided color reference. The degradation level attributed depends on the color of the strip, ranging from 0 (strip blue, no acetic acid detected) to 3 (strip yellow, acetic acid concentration in the box > 20 ppm). Each degradation level is correlated with a range of acetic acid vapor concentration.

The developed ZnO/PANI-based sensors showed good sensitivity comparing to ZnO-based gas sensors, based on resistive metal oxide nanostructures [6,7,29]. As published in Refs. [6,7,29], the resistive sensors has wide working range with fast response and recovery time Table 2. Fast recovery in resistive type acetic acid gas sensor can be attributed their high operating temperatures. However, sensors operating at high temperature consume more energy and cannot be used to detect gases at archives where nitrocellulose films stored due to their explosive nature.

In monitoring of cellulose degradation, the key parameters are operation at room temperature and fast response. Therefore, the proposed optical sensors can be used for this purpose.

## 4. Conclusions

The results presented in this work show for the first time that ZnO/PANI-based nanocomposites are good candidates for the determination of acetic acid at room temperature based on photoluminescence measurements. The results of the photoluminescence and measurements of these composites exposed to the acetic acid vapors show that photoluminescence decrease with increasing the samples concentration. Here developed ZnO/PANI-based sensor showed good sensitivity to acetic acid in the range of 1–13 ppm, with acceptable response and recovery times suitable for the monitoring of acetic acid.

A new miniaturized sensing system based on ZnO/PANI sensing layer prototype was developed. The prototype combines LED (UV) and a fiber optic measurements system with photoluminescence ZnO/PANI sensing element. The sensor prototype collected the photoluminescence signal *via* optical fiber with high yield. The developed sensor can be of practical interest for monitoring vinegar and for precaution in protection of the cultural heritage against acetic acid production during the degradation of acetate cellulose films, since their storage is an important task related to protection and conservation of cultural heritage.

## Acknowledgements

The research leading to these results has received funding from the European Union's Horizon 2020 Program: NMBP-35-2017 - Innovative solutions for the conservation of 20th century cultural heritage (Grant agreement ID: 760801), and MSCA-RISE-2017 - Research and Innovation Staff Exchange H2020-EU.1.3.3-Grant agreement ID: 778157 (CanBioSe) to MT. We would like to thank Fratelli Alinari Istituto di Edizioni Artistiche I.D.E.A Spa. the oldest company in the world in the field of photography and communication through images, for their support in providing film samples.

## References

- [1] R. Viter, I. Iatsunskiy, Metal oxide nanostructures in sensing, *Nanomater. Des. Sens. Appl.* 2019, <https://doi.org/10.1016/b978-0-12-814505-0.00002-3>.
- [2] M. Sanchez-Sala, O. Vallcorba, C. Domingo, J.A. Ayllón, Acetic acid as a solvent for the synthesis of metal-organic frameworks based on trimesic acid, *Polyhedron* 170 (2019) 458–462, <https://doi.org/10.1016/J.POLY.2019.06.017>.
- [3] J.A.M. Leyva, J.L.H. Hidalgo de Cisneros, D.G. Gomez de Barreda, A coated piezoelectric crystal sensor for acetic acid vapour determination, *Talanta* 40 (1993) 1725–1729, [https://doi.org/10.1016/0039-9140\(93\)80090-E](https://doi.org/10.1016/0039-9140(93)80090-E).
- [4] L. Teodonio, M. Missori, D. Pawcenis, J. Lojewska, F. Valle, Nanoscale analysis of degradation processes of cellulose fibers, *Micron* 91 (2016) 75–81, <https://doi.org/10.1016/J.MICRON.2016.07.013>.
- [5] K. Curran, A. Možir, M. Underhill, L.T. Gibson, T. Fearn, M. Strlič, Cross-infection effect of polymers of historic and heritage significance on the degradation of a cellulose reference test material, *Polym. Degrad. Stab.* 107 (2014) 294–306, <https://doi.org/10.1016/J.POLYDEGRADSTAB.2013.12.019>.
- [6] C. Wang, S. Ma, A. Sun, R. Qin, F. Yang, X. Li, F. Li, X. Yang, Characterization of electrospun Pr-doped ZnO nanostructure for acetic acid sensor, *Sens. Actuators B Chem.* 193 (2014) 326–333, <https://doi.org/10.1016/J.SNB.2013.11.058>.
- [7] L. Cheng, S.Y. Ma, T.T. Wang, J. Luo, X.B. Li, W.Q. Li, Y.Z. Mao, D.J. Gz, Highly sensitive acetic acid gas sensor based on coral-like and Y-doped SnO<sub>2</sub> nanoparticles prepared by electrospinning, *Mater. Lett.* 137 (2014) 265–268, <https://doi.org/10.1016/J.MATLET.2014.09.040>.
- [8] E. Asijati, B. Kuswandi, N.F. Arifah, Y.I. Kurniawati, A.A. Gani, Non-invasive optical chemical sensor based on polyaniline films for detection of ammonia and acetic acid solutions, 2005 Asian Conf. Sensors Int. Conf. New Tech. Pharm. Biomed. Res. - Proc. 2005, <https://doi.org/10.1109/ASENSE.2005.1564518>.
- [9] M.G. Guillén, F. Gámez, T. Lopes-Costa, J.R. Castro-Smirnov, R. Wannemacher, J. Cabanillas-González, J.M. Pedrosa, Amplified spontaneous emission in action: sub-ppm optical detection of acid vapors in poly[2-methoxy-5-(2-ethylhexyloxy)-1,4-phenylenevinylene] thin films, *Sens. Actuators B Chem.* 255 (2018) 1354–1361, <https://doi.org/10.1016/J.SNB.2017.08.136>.
- [10] M. Weber, J.Y. Kim, J.H. Lee, J.H. Kim, I. Iatsunskiy, E. Coy, P. Miele, M. Bechelany, S.S. Kim, Highly efficient hydrogen sensors based on Pd nanoparticles supported on boron nitride coated ZnO nanowires, *J. Mater. Chem. A* (2019), <https://doi.org/10.1039/c9ta00788a>.
- [11] M. Weber, J.H. Kim, J.H. Lee, J.Y. Kim, I. Iatsunskiy, E. Coy, M. Drobek, A. Julbe, M. Bechelany, S.S. Kim, High-performance nanowire hydrogen sensors by exploiting the synergistic effect of Pd nanoparticles and metal-organic framework membranes, *ACS Appl. Mater. Interfaces* (2018), <https://doi.org/10.1021/acsami.8b12569>.
- [12] A.N. Zolotko, N.I. Poletaev, Y.I. Vovchuk, Gas-disperse synthesis of metal oxide particles, *Combust. Explos. Shock Waves* 51 (2015), <https://doi.org/10.1134/S0010508215020094>.
- [13] A. Kausaitė, A. Ramanavičienė, A. Ramanavičius, Polyaniline synthesis catalysed by glucose oxidase, *Polymer (Guildf)* (2009), <https://doi.org/10.1016/j.polymer.2009.02.013>.
- [14] R. Viter, V. Khranovskyy, N. Starodub, Application of room temperature photoluminescence from ZnO nano-rods for Salmonella detection, *IEEE Sens. J.* 14 (2014) 2028–2034 [http://ieeexplore.ieee.org/xpls/abs\\_all.jsp?arnumber=6750731](http://ieeexplore.ieee.org/xpls/abs_all.jsp?arnumber=6750731), Accessed date: 16 September 2014.
- [15] E.M. Elnaggar, K.I. Kabel, A.A. Farag, A.G. Al-Gamal, Comparative study on doping of polyaniline with graphene and multi-walled carbon nanotubes, *J. Nanostructure Chem.* (2017), <https://doi.org/10.1007/s40097-017-0217-6>.
- [16] R.K. Sonker, B.C. Yadav, A. Sharma, M. Tomar, V. Gupta, Experimental investigations on NO<sub>2</sub> sensing of pure ZnO and PANI-ZnO composite thin films, *RSC Adv.* (2016), <https://doi.org/10.1039/c6ra07103a>.
- [17] R. Viter, K. Jekabsons, Z. Kalnina, N. Poletaev, S.H. Hsu, U. Riekstina, Bioanalytical system for detection of cancer cells with photoluminescent ZnO nanorods, *Nanotechnology* 27 (2016) 465101, <https://doi.org/10.1088/0957-4484/27/46/465101>.
- [18] A. Ramanavičius, N. Ryskevicius, Y. Oztekin, A. Kausaitė-Minkstimiene, S. Jursenas, J. Baniukevič, J. Kirlyte, U. Bubniene, A. Ramanavičienė, Immunosensor based on fluorescence quenching matrix of the conducting polymer polypyrrole, *Anal. Bioanal. Chem.* (2010), <https://doi.org/10.1007/s00216-010-4265-8>.
- [19] A. Ramanavičius, N. Kurilcik, S. Jursenas, A. Finkelsteinas, A. Ramanavičienė, Conducting polymer based fluorescence quenching as a new approach to increase the selectivity of immunosensors, *Biosens. Bioelectron.* (2007), <https://doi.org/10.1016/j.bios.2007.06.013>.
- [20] D.D. Le, T.N.N. Nguyen, D.C.T. Doan, T.M.D. Dang, M.C. Dang, Fabrication of interdigitated electrodes by inkjet printing technology for application in ammonia sensing, *Adv. Nat. Sci. Nanosci. Nanotechnol.* (2016), <https://doi.org/10.1088/2043-6262/7/2/025002>.
- [21] R. Viter, I. Iatsunskiy, Optical spectroscopy for characterization of metal oxide nanofibers, *Handb. Nanofibers*, 2019, [https://doi.org/10.1007/978-3-319-53655-2\\_10](https://doi.org/10.1007/978-3-319-53655-2_10).
- [22] R. Viter, M. Savchuk, I. Iatsunskiy, Z. Pietralik, N. Starodub, N. Shpyrka, A. Ramanavičienė, A. Ramanavičius, Analytical, thermodynamical and kinetic characteristics of photoluminescence immunosensor for the determination of Ochratoxin A, *Biosens. Bioelectron.* 99 (2018) 237–243, <https://doi.org/10.1016/j.bios.2017.07.056>.
- [23] R. Viter, M. Savchuk, N. Starodub, Z. Balevičius, S. Tumenas, A. Ramanavičienė, D. Jevdokimovs, D. Erts, I. Iatsunskiy, A. Ramanavičius, Photoluminescence immunosensor based on bovine leukemia virus proteins immobilized on the ZnO nanorods, *Sens. Actuators B Chem.* (2019), <https://doi.org/10.1016/j.snb.2019.01.054>.
- [24] S.L. Patil, M.A. Chougule, S.G. Pawar, S. Sen, A.V. Moholkar, J.H. Kim, V.B. Patil, Fabrication of polyaniline-ZnO nanocomposite gas sensor, *Sensors and Transducers* 134 (11) (2011) 120–131.
- [25] S.B. Kondawar, P.T. Patil, S.P. Agrawal, Chemical vapour sensing properties of electrospun nanofibers of polyaniline/ZnO nanocomposites, *Adv. Mater. Lett.* (2014), <https://doi.org/10.5185/amlett.2014.amwc.1037>.
- [26] M. Das, D. Sarkar, One-pot synthesis of zinc oxide - polyaniline nanocomposite for fabrication of efficient room temperature ammonia gas sensor, *Ceram. Int.* (2017), <https://doi.org/10.1016/j.ceramint.2017.05.159>.
- [27] H. Xu, X. Chen, J. Zhang, J. Wang, B. Cao, D. Cui, NO<sub>2</sub> gas sensing with SnO<sub>2</sub>-ZnO/PANI composite thick film fabricated from porous nanosolid, *Sens. Actuators B Chem.* (2013), <https://doi.org/10.1016/j.snb.2012.09.060>.
- [28] J. Chauhan, Preparation and characterization of polyaniline/ZnO composite sensor, *J. Nanomedicine Res.* (2017), <https://doi.org/10.15406/jnmr.2017.05.00104>.
- [29] V. Khorramshahi, J. Karamdel, R. Yousefi, High acetic acid sensing performance of Mg-doped ZnO/rGO nanocomposites, *Ceram. Int.* (2019), <https://doi.org/10.1016/j.ceramint.2018.12.205>.
- [30] L. Zhang, Y. Li, Q. Zhang, H. Wang, Well-dispersed Pt nanocrystals on the hetero-structured TiO<sub>2</sub>/SnO<sub>2</sub> nanofibers and the enhanced photocatalytic properties, *Appl. Surf. Sci.* 319 (2014) 21–28, <https://doi.org/10.1016/j.apsusc.2014.07.199>.
- [31] Z. Cheng, S. Zhou, T. Chen, Y. Dong, W. Zhang, X. Chu, Acetic acid gas sensors based on Ni<sup>2+</sup> doped ZnO nanorods prepared by using the solvothermal method, *J. Semicond.* (2012), <https://doi.org/10.1088/1674-4926/33/11/112003>.
- [32] J. Fu, L. Zhang, Sensing parts per million level ammonia and parts per billion level acetic acid in the gas phase by common black film with a fluorescent pH probe, *Anal. Chem.* (2018), <https://doi.org/10.1021/acs.analchem.7b04347>.

**Dr. Mehmet Turemis** received his M.Sc. degree in biochemistry in 2010 from Ege Universitesi, Izmir, Turkey and a PhD degree in biotechnology from the Università della Tuscia of Viterbo within ITN Marie Curie project. At present he is working as experienced researcher at Biosensor S.r.l. His research interests focus on the development and characterization of biosensors and their applications in the field of medicine, water treatment, and biotechnologies.

**Dr. Maria Teresa Giardi** is associated researcher at the National Council of Research (CNR) in Rome, Italy. Her background is in organic-industrial chemistry and she has extensive experience in biochemistry; development of signal transduction systems for optical and electrochemical biosensors; protein stabilization and utilization in biosensor design. She has worked in various research institutions and research and development companies in both Europe and the USA. She is a supervisor or coordinator of a number of national and international projects in the field of biosensors: European Agency projects Frame V, VI, VII; European Space Agency projects involving space flights to ISS.

**Dr. Daniele Zappi** achieved Master's Degree cum Laude in Analytical Chemistry with a thesis titled "Preparation and characterization of electrochemical biosensors based on fourth-generation ionic liquids and enzymes" at University "La Sapienza" of Rome. At present he is working at Biosensor s.r.l. His research focus is on the development of electrochemical sensors and their optimization for analysis on complex matrices.

**Dr. Giovanni Basile** has a solid multi-year experience in industrial research project management. He got his start in biosensor research in optical sensors for the mechanical industry after his degree at the University of Rome. His current research is focused on the development of environmental and biomedical sensors using fluorescence spectroscopy. Giovanni is a proponent of multidisciplinary engineering design, and thus integrates microfluidics, data science, photonics, and nanotechnology into his research. He is co-inventor of various patents and he has successfully coordinated three European Projects in the Frame VII and H2020.

**Prof. Dr. Almira Ramanavičienė**, is a head of Nanotechnas – Centre for Nanotechnology and Materials Science at the Faculty of Chemistry and Geosciences of Vilnius University, and head of biosensor research groups at State Research Institute Centre for Innovative Medicine, Lithuania. She received her PhD degree in biomedicine in 2002 from the Institute of Immunology of Vilnius University. In 2008 she completed habilitation procedure in Physical Sciences at Vilnius University. Prof. dr. Almira Ramanavičienė is serving as expert for the European Commission and other international and national foundations. She has comprehensive experience in the field of biosensors and immunosensor development focusing on different surface modification techniques and various detection methods.

**Prof. Habil. Dr. Arunas Ramanavičius** is a professor and head of Department of Physical Chemistry at faculty of Chemistry of Vilnius University. He is also leading the laboratory of NanoTechnology at Research Center of Physical Sciences and Technologies. Prof. Arunas Ramanavičius is a member of Lithuanian Academy of sciences. In 1998 he



received PhD degree and in 2002 doctor habilitus degree from Vilnius University. Prof. A. Ramanavicius is serving as expert-evaluator in Horizon 2020 program coordinated by European Commission and he is technical advisor of many foundations located in European and non-European countries. He has research interests in various aspects of nanotechnology, bionanotechnology, nanomaterials, biosensors, bioelectronics, biofuel cells and MEMS based analytical devices. He was a national coordinator of several nanotechnology-related COST actions.

**Mr. Aleksandrs Kapralovs** Aleksandrs Kapralovs has graduated from Riga Technical college in 1980. He got a specialty in mechanical engineering. Since 1984, he has worked in ALFA company, working on industrial solutions for glass ware, gas supply systems, vacuum technique prototypes and high temperature processes. Since 2003, he has

obtained permanent position of engineer at Institute of Atomic Physics and Spectroscopy, University of Latvia. In Institute of Atomic Physics and Spectroscopy his main activities are support in mechanical engineering, glass ware, gas supply systems and prototypes of measurements systems.

**Dr. Roman Viter** got a MSc degree in physic at Odessa National I.I. Mechnikov University, Odessa, Ukraine in 2000. He got his PhD at Odessa National I.I. Mechnikov University, Odessa, Ukraine in 2011. Since 2014 he has obtained a position of Senior researcher at Institute of Atomic Physics and Spectroscopy, University of Latvia. He is a coordinator of Latvian and H2020 projects. He is a supervisor of MSc, PhD and postdoc projects. His main research is focused on development and characterization of photonic nanomaterials for applications in optical sensors and biosensors.